Journal of Machine Engineering, 2024, Vol. 24
ISSN 1895-7595 (Print) ISSN 2391-8071 (Online)

Received*: 15 May 2024* / Accepted: *06 June 2024* / Published online: *30 August 2024*

control, machine tool,
thermal error,
thermal modal analysis

Patrick PÖHLMANN[1*],
Jens MÜLLER[1],
Steffen IHLENFELDT[1,2.]

STRATEGY FOR COMPENSATION OF THERMALLY INDUCED DISPLACEMENTS IN MACHINE STRUCTURES USING DISTRIBUTED TEMPERATURE FIELD CONTROL

Thermal deformation is a major source of machining errors in modern machine tools. In addition to optimising the machine structure, correcting the axis position values in the numerical control is a common measure to reduce these errors. Another possibility is to directly influence the temperature field of the machine tool in the process, which requires a complex thermo-elastic modelling approach as well as appropriate thermal actuation and measurement capabilities. This paper presents a strategy for controlling the temperature field based on the eigenmodes of the thermal system. The various aspects of the concept are explained using a finite element model of an exemplary structural component. The basis is the modal analysis of the thermal system, which allows the temperature field to be described by independent discrete states. In addition to the placement of thermal sensors and actuators, this work focuses on the design of a suitable control approach. Transient simulation results are used to clearly demonstrate the performance of this method.

1. INTRODUCTION

A significant proportion of geometric machining errors in modern machine tools are caused by thermal processes [1]. Local changes in the temperature field occur in the machine frame due to the power dissipation of the drives and the machining process. As a result, the machine structure deforms depending on its geometric design and the thermal expansion coefficient of the material. The associated displacement of reference points, particularly the tool centre point (TCP), leads to geometric errors in the machining process.

A significant challenge associated with thermal displacements is that they undergo continuous changes until a thermal steady state is reached. Depending on the design of the machine tools, this period can exceed the machining time of a single part, which can result in processing errors.

[1] Institute of Mechatronic Engineering, Chair of Machine Tools Development and Adaptive Controls, Dresden University of Technology, Germany
[2] Department for Cyber-Physical Production Systems (CPPS), Fraunhofer Institute for Machine Tools and Forming Technology IWU, Germany
[*] E-mail: patrick.poehlmann@tu-dresden.de
https://doi.org/10.36897/jme/189765

For this reason, the reduction of thermally induced errors is the subject of much research. This starts with the thermal optimisation of mechanical assemblies, e.g. through thermo-symmetric design, which also includes heat sources (e.g. drives). Other possibilities include the targeted reduction and insulation of heat sources on the machine structure [3]. Since other aspects such as statics, dynamics and function also play a role in machine design, thermal design is only one aspect and the scope for action is limited.

A commonly used method is the use of correction values in the machine control system, which requires the use of appropriate error models. The challenges here are the definition of the model, its parametrisation (see [4]), which is usually difficult to determine experimentally, and last but not least the measurement of state and process variables at runtime. One possible approach is to use empirical models derived from measured data such as temperature, strain and displacement. Methods such as linear and non-linear regression functions (e.g. [5, 6]), thermal transfer functions (e.g. [7, 8]) or neural networks (e.g. [9, 5, 10]) are used for this purpose. The disadvantages of empirical methods are that a high experimental effort is often required to collect regression and training data [10], and it must be ensured that the scenarios occurring during operation can be represented by the data collected in the experiments. Parametric models, on the other hand, can be used to model scenarios and states that have not been measured. For easily discretised objects, node models often provide a simple solution. For complex structures, numerical solutions such as the finite element method (FEM) are usually used. Thermal modal analysis (see [11, 12]) is a method of analysing the thermal properties of a structure. It solves the eigenvalue problem of the underlying linear system. In the case of a discrete FE model, the system consisting of a large number of coupled degrees of freedom can be transformed into a description of independent single-variable systems (thermal modes) of the same number by modal transformation (see Section 2).

Although central cooling systems are often used, they are unable to counteract the deformation caused by temperature gradients. This requires local cooling capacity tailored to the needs of the application. To achieve this, the system must have individually controllable actuators (heating/cooling system). This results in a complex multivariable system with distributed parameters. In addition to the correction by the machine control, approaches to compensate for thermally induced deformations using additional heat sources are known [13, 14, 8]. The modal control technique is mainly known for elastic mechanical systems (see [15, 16, 17]). Extensive analytical and practical investigations of thermal modal control in distributed parametric systems have been carried out by Morishima using the example of a rectangular plate [14]. In the case of a three-dimensional body, however, this approach is very limited because the temperature field inside the body cannot be measured by sensors. Instead, thermal states must be estimated in real time using discrete temperature measurements. This paper presents a strategy for applying modal control of the temperature field to a spatial machine structure. This approach simplifies parametrisation, as it enables the design of an independent single-variable controller for each thermal mode to be controlled. By actively stabilising the temperature field, the aim is to reduce the thermally induced shift of the operating point of a machine.

Section 2 first presents the modal analysis of a discrete linear thermal system. The example component considered in this work and the associated FE model are described. This

is followed by the application of thermal modal analysis and its results in Section 3. Section 4 deals with the concept of modal control. PI controllers for each degree of freedom with simple parametrisation are used for illustration. Based on the model and the control used, a transient simulation is performed in Section 5 and the results are summarised.

2. THERMAL MODAL ANALYSIS

The thermal modal analysis is briefly illustrated below. The basis is a system of N linear differential equations

$$\boldsymbol{C}\dot{\boldsymbol{T}}(t) + \boldsymbol{K}\boldsymbol{T}(t) = \boldsymbol{q}(t), \tag{1}$$

with the vectors of the temperatures $\boldsymbol{T}(t)$ and thermal loads $\boldsymbol{q}(t)$ as well as the matrices of the thermal capacities $\boldsymbol{C}$ and the conductances $\boldsymbol{K}$. For spatially distributed bodies, this discrete representation can be set up using FE analysis, for example. The corresponding eigenvalue equation follows from the solution approach $\boldsymbol{T}(t) = \boldsymbol{\phi}\hat{\theta}\mathrm{e}^{\lambda t}$ of the load-free system (1) ($\boldsymbol{q}(t) = 0$):

$$(\lambda\boldsymbol{C} + \boldsymbol{K})\boldsymbol{\phi} = 0, \tag{2}$$

whose solution is formed from the eigenvalues λ_i $(i = 1 \dots N)$ and the corresponding eigenvectors $\boldsymbol{\phi}_i$. The modal matrix $\boldsymbol{\Phi} = (\boldsymbol{\phi}_1 \cdots \boldsymbol{\phi}_N)$ consisting of the eigenvectors can be used to convert the physical state space into the modal state space:

$$\boldsymbol{T}(t) = \sum \boldsymbol{\phi}_i \theta_i(t) = \boldsymbol{\Phi}\boldsymbol{\theta}(t). \tag{3}$$

If this transformation is applied to (1) and multiplied from the left by $\boldsymbol{\Phi}^{\mathrm{T}}$, the modal system representation is obtained

$$\boldsymbol{\Phi}^T\boldsymbol{C}\boldsymbol{\Phi}\dot{\boldsymbol{\theta}}(t) + \boldsymbol{\Phi}^T\boldsymbol{K}\boldsymbol{\Phi}\boldsymbol{\theta}(t) = \boxed{\boldsymbol{\Gamma}\left(\dot{\boldsymbol{\theta}}(t) + \boldsymbol{\Lambda}\boldsymbol{\theta}(t)\right) = \boldsymbol{\xi}(t)} = \boldsymbol{\Phi}^T\boldsymbol{q}(t), \tag{4}$$

where $\boldsymbol{\xi}(t)$ represents the modal load transformed by $\boldsymbol{\Phi}^{\mathrm{T}}$. A special feature of this particular transformation is that the matrix of modal capacities $\boldsymbol{\Gamma}$ and the matrix of eigenvalues $\boldsymbol{\Lambda} = \mathrm{diag}(\lambda_1 \cdots \lambda_N)$ consists of N independent first-order systems (in the following: thermal modes), which are coupled to the physical loads $\boldsymbol{q}(t)$ and states $\boldsymbol{T}(t)$ via the static transformations $\boldsymbol{\Phi}$ and $\boldsymbol{\Phi}^{\mathrm{T}}$.

Furthermore, it is assumed that the thermal processes occur at a sufficiently slow rate to allow the deformation of the structure to be represented by the stiffness matrix $\boldsymbol{E}$ and the thermo-elastic coupling matrix $\boldsymbol{A}$:

$$\boldsymbol{E}\boldsymbol{u} + \boldsymbol{A}\boldsymbol{T} = \boldsymbol{f}\,. \tag{5}$$

If there are no mechanical loads $\boldsymbol{f}$, the displacement $\boldsymbol{u}$ is calculated by a static transformation of the temperature field $\boldsymbol{T}$:

$$\boldsymbol{u} = \boldsymbol{E}^{-1}\boldsymbol{A}\boldsymbol{T} = \boldsymbol{E}^{-1}\boldsymbol{A}\boldsymbol{\Phi}\boldsymbol{\theta} = \boldsymbol{\Psi}\boldsymbol{\theta}\,. \tag{6}$$

The matrix $\boldsymbol{\Psi} = \boldsymbol{E}^{-1}\boldsymbol{A}\boldsymbol{\Phi}$ represents a mapping of the modal thermal state onto the displacement field of the structure. Accordingly, the columns of $\boldsymbol{\Psi}$ can be interpreted as modal displacement functions (deformation shape).

3. Structural example and model

The machine tool component shown in Fig. 1 (left) forms the exemplary basis for the following analyses. This is a column structure with a vertical axis of motion. The slide, guided by guiding rails, is driven by a ball screw and a servo motor.

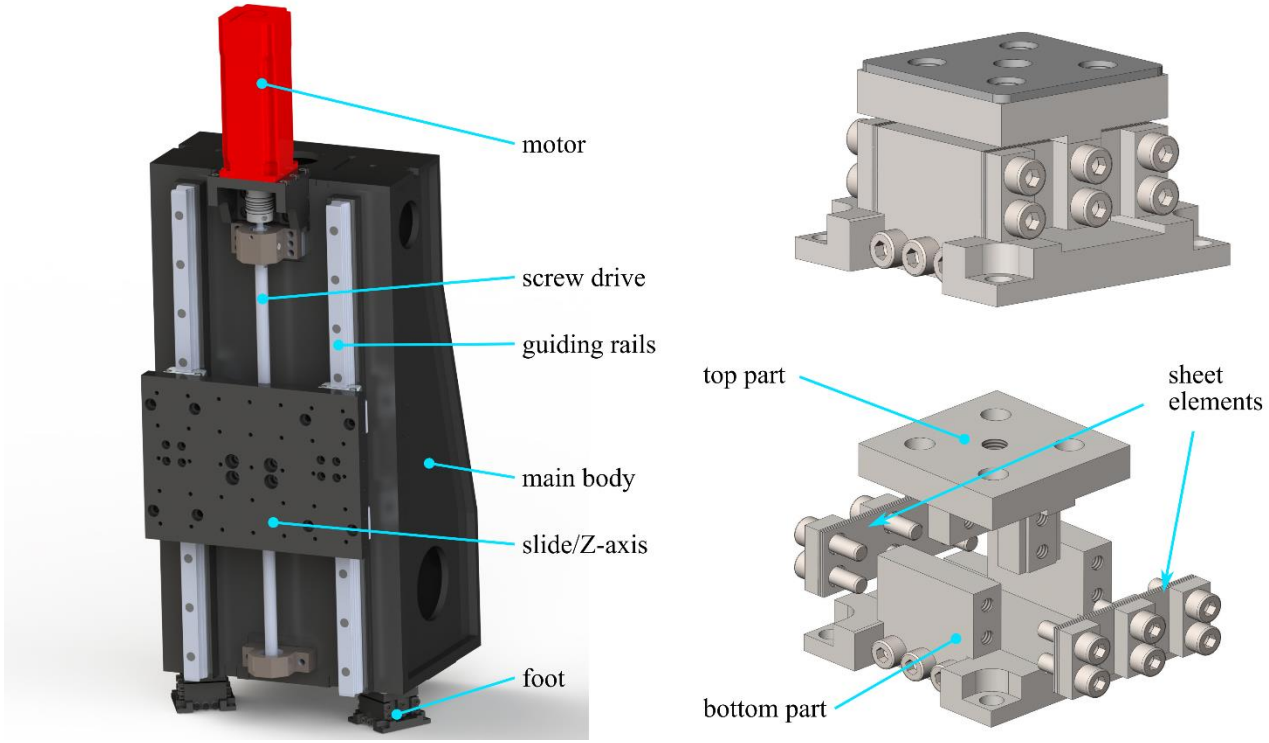

Fig. 1. CAD model of the test rig (left) and the construction of the foot elements (right)

The properties of the mechanical and thermal boundary conditions have a significant influence on the thermoelastic behaviour. As this is essentially a concept paper, the boundary conditions are initially described using simplified linear approaches. Linearisation is necessary anyway for the calculation of thermal modes. The heat transfer to the ambient air is modelled using surface related conductance values.

One particular aspect is the positioning of the structure. If the entire structure is very rigidly attached to the base, a strong interaction will occur. To minimise the uncertainties, the structure was mounted on three specially designed machine feet (Fig. 1, right). Each foot is designed to be compliant with forces acting in a specific direction within the X-Y plane. This

is achieved through the use of spring steel plates, which act as solid links. The concept of using packages of spring steel plates as joints has been presented in previous work [18]. As the feet are at an angle of 120° to each other, the three degrees of freedom in the X-Y plane are clearly defined. For example, if the structure experiences an overall temperature change, it will expand in relation to its centre, keeping the reaction forces of the feet small.

Based on the design data, an FE model of the structure is created below using ANSYS software. Figure 2 shows the FE model of the frame without any attached components. In addition, details of the geometry have been simplified to allow efficient meshing with hexahedral volume elements. The foot components are investigated in separate thermal and mechanical analyses. The aim is to determine discrete equivalent parameters for heat conduction and a six-dimensional stiffness matrix. Only these equivalent parameters are then integrated into the model of the overall structure. Detailed temperature and deformation fields within the feet are not modelled in this way.

The MATLAB and Simulink tools are used to perform the analyses that are not covered by the ANSYS simulation environment. In addition to the matrices $\boldsymbol{C}$, $\boldsymbol{K}$, $\boldsymbol{E}$ and $\boldsymbol{A}$ introduced in (1) and (6), the surface information $\boldsymbol{w}_{\mathrm{A},i}$ required to apply the boundary conditions is also generated and exported. This vector is used to evenly distribute a discrete heat flow $q_{\mathrm{A},i}$ at surface i caused by a boundary condition to the resulting thermal loads at the individual nodes:

$$\boldsymbol{q}_i = \boldsymbol{w}_{A,i} q_{A,i}. \tag{7}$$

The areas where thermal loads are to be applied are marked in red in Fig. 2. The point *P*, marked at the top of the front, is used as a reference point for the rest of the paper. The selected areas also serve as temperature measurement points. In this way the actuators and sensors are in a collocated arrangement.

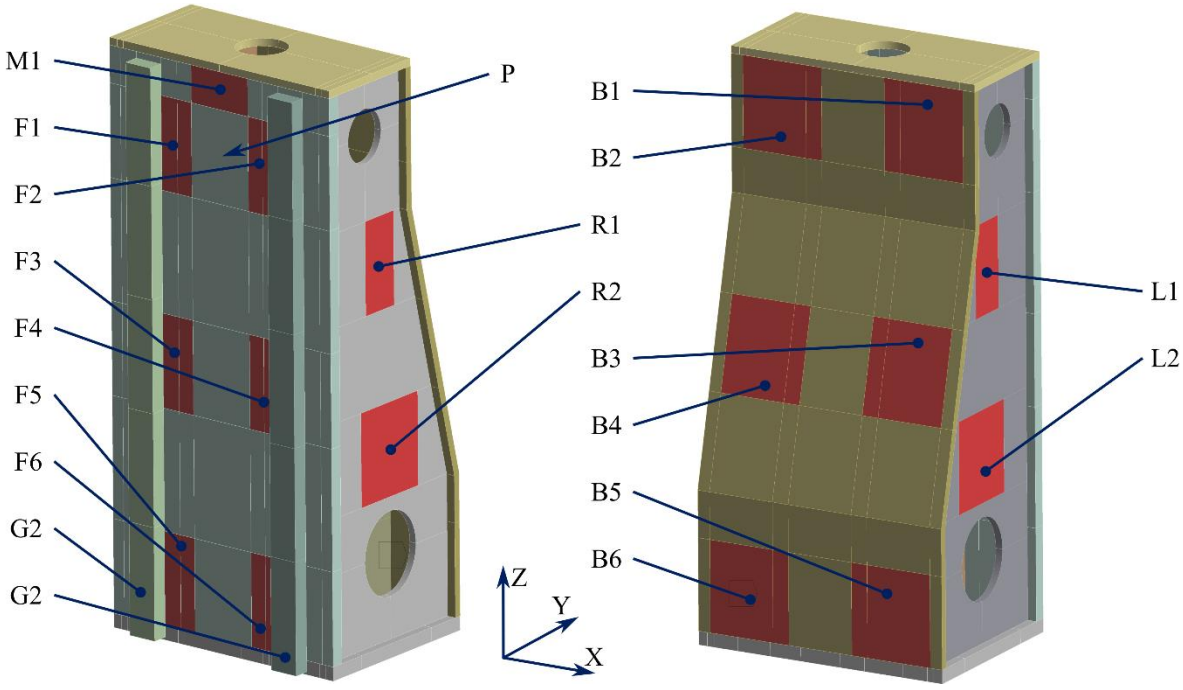

Fig. 2. FE model and faces for thermal loads and actuators

Thermal modal analysis is illustrated below using this structural example. Figure 3 shows the temperature distribution $\boldsymbol{\phi}_i$ of the first eight thermal modes resulting from solving (2). These are scaled to the value range between -1 and 1 for illustrative purposes. The associated thermal time constants $\tau_i = 1/\lambda_i$ are listed in the following Table 1. Figure 4 shows the time constants of the first 500 modes. The first mode has the most uniform temperature shape and a high time constant τ. It describes a uniform heat flow from the body to the surroundings. As the largest heat flow is through the feet, the relative temperature is lowest here. In the other modes, the time constant decreases rapidly and the gradients of the temperature field increase.

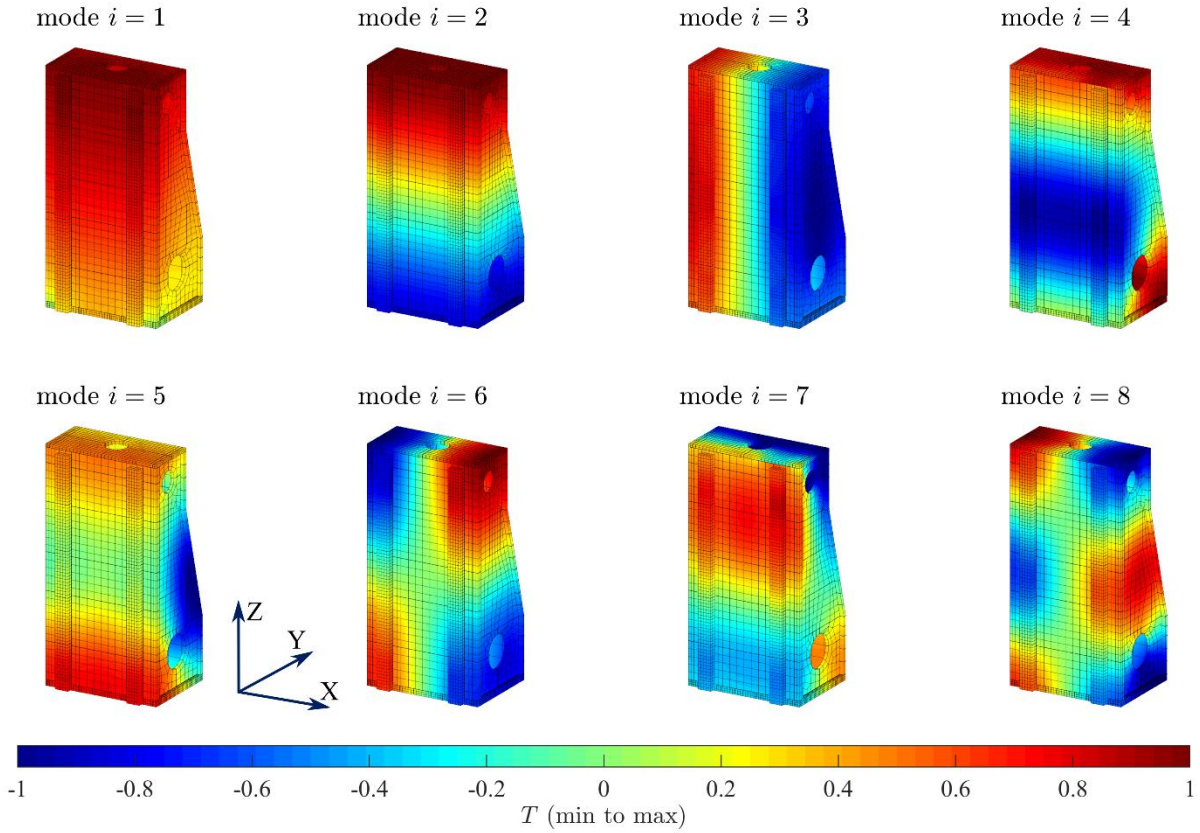

Fig. 3. Thermal mode shapes of the structural example

Table 1. List of the first 18 time constants $\tau = 1/\lambda$

mode i	τ (min)	mode i	τ (min)	mode i	τ (min)
1	280.7	7	7.64	13	4.69
2	39.5	8	6.84	14	4.13
3	16.7	9	6.41	15	3.98
4	12.5	10	5.57	16	3.59
5	11.6	11	4.99	17	3.47
6	10.9	12	4.91	18	3.20

The deformation fields $\boldsymbol{\psi}_i$ caused by the modal temperature fields can be calculated using (6). Figure 5 shows these for the first eight modes with exaggerated scaling. The colour

indicates the magnitude of the displacement $|u| = \sqrt{u_x^2 + u_y^2 + u_z^2}$ and is normalised to values between 0 and 1. Figure 6 shows the displacement of the reference point *P* for each coordinate direction in a diagram. The unit m/K here refers to the modal amplitude. This is difficult to interpret as the scaling of the eigenvectors $\boldsymbol{\phi}_i$ also plays a role here. In this example, $\boldsymbol{\phi}_i$ has been normalised to a value of 1. The amount of excitation of a thermal mode in typical load scenarios also plays an important role in the assessment for a practical application.

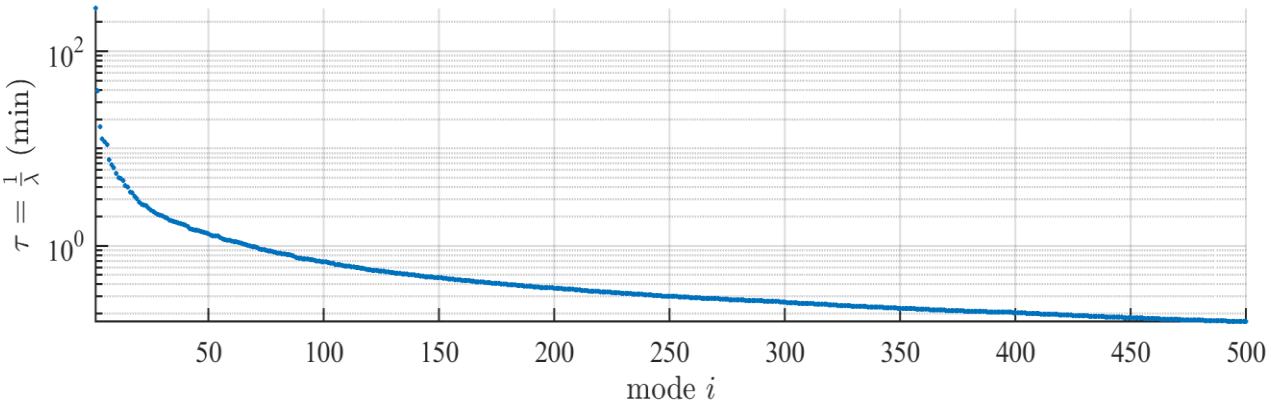

Fig. 4. The first 500 time constants $\tau = 1/\lambda$

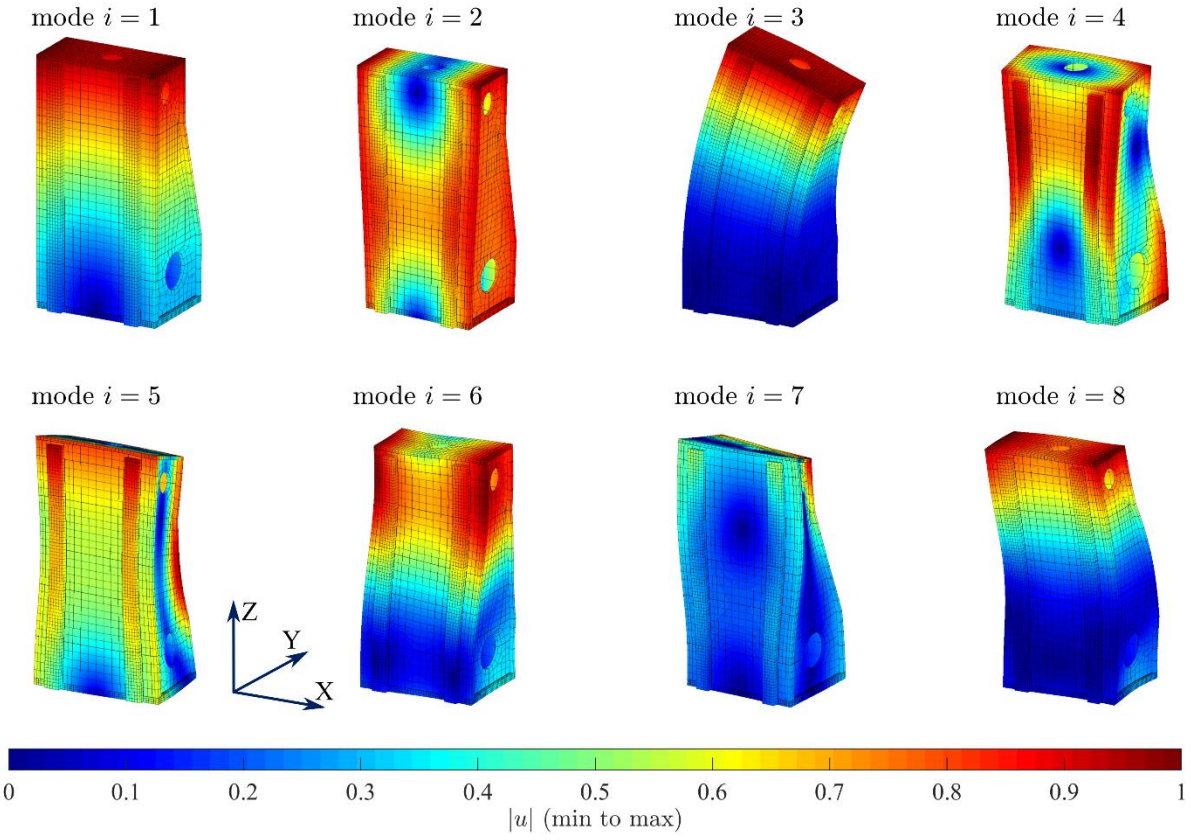

Fig. 5. Deformation shapes $\boldsymbol{\psi}_i$ corresponding to the first thermal modes

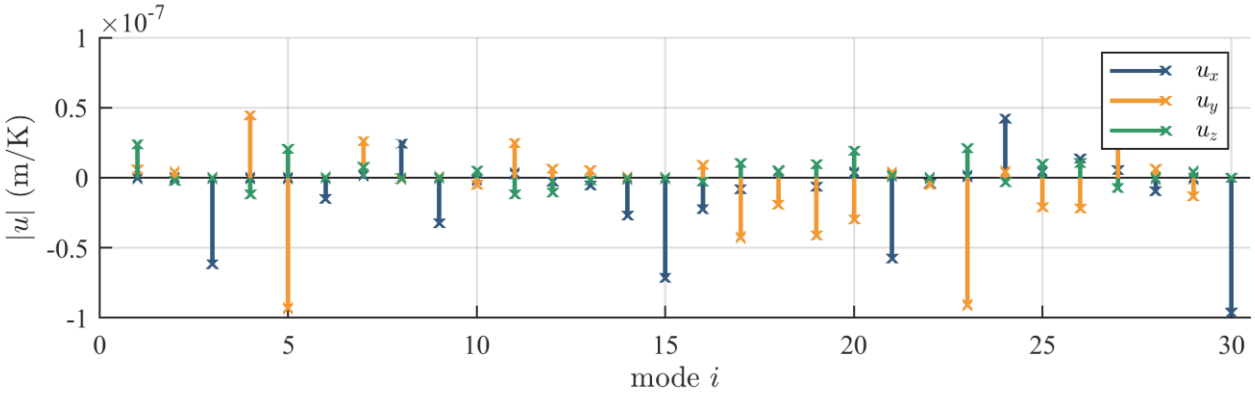

Fig. 6. Deformation of the reference point *P* corresponding to the first thermal modes

4. Modal Control Example

The basic idea of mode control is to use a separate, independent control law for each thermal mode. This ensures a simple procedure for parameter setting, especially as the behaviour of each thermal mode corresponds to a PT1 transfer function. In this example, simple PI controllers are used for control:

$$\bar{\xi}_{C,i}(t) = k_{P,i}\left(\bar{\theta}_{SP,i}(t) - \bar{\theta}_{C,i}(t)\right) + k_{I,i}\int\left(\bar{\theta}_{SP,i}(t) - \bar{\theta}_{C,i}(t)\right)dt. \tag{8}$$

The setpoint $\bar{\theta}_{\mathrm{SP},i}(t)$ and an estimated modal temperature $\bar{\theta}_{\mathrm{C},i}$ which is calculated from discrete measured temperature values $\boldsymbol{T}_{\mathrm{S}}$ using a transformation matrix $\boldsymbol{X}_{\mathrm{S}}$, are used as the input to the controller:

$$\bar{\boldsymbol{\theta}}_C = \boldsymbol{X}_S\boldsymbol{T}_S\,. \tag{9}$$

The matrix $\boldsymbol{X}_{\mathrm{S}}$ is known from mechanical applications as a modal filter [16]. To calculate it, a submatrix $\boldsymbol{\Phi}_{\mathrm{C,S}}$ of the full modal matrix is formed by using the columns of the modes to be controlled and the rows corresponding to the temperature measurements $\boldsymbol{T}_{\mathrm{S}}$, which are a subset of all physical temperatures $\boldsymbol{T}$ in (3). As there are as many sensors in this case as there are modes to be controlled, the calculation is performed by inversion:

$$\boldsymbol{X}_S = \left(\boldsymbol{\Phi}_{C,S}\right)^{-1}. \tag{10}$$

The desired heat flows of the actuators $\boldsymbol{q}_{\mathbf{A}}$ are calculated in a similar way from the desired modal controller outputs ξ_{C}:

$$\boldsymbol{q}_A = \boldsymbol{X}_A\bar{\boldsymbol{\xi}}_C\,. \tag{11}$$

$\boldsymbol{X}_{\mathrm{A}}$ is also obtained from the modal matrix, using the rows of the corresponding actuators $\boldsymbol{q}_{\mathrm{A}}$, which are a subset of all thermal loads $\boldsymbol{q}$ in (4):

$$\boldsymbol{X}_A = \left(\boldsymbol{\Phi}_{C,A}^T\right)^{-1}. \tag{12}$$

In this example, a FE model is used and each actuator is connected to multiple nodes. Therefore, it is necessary to consider that several rows of $\boldsymbol{\Phi}$ must be aggregated into a single

row of $\boldsymbol{\Phi}_{\mathrm{C,A}}$ for each actuator, utilising appropriate weightings $\boldsymbol{w}_{\mathrm{A}}$ (see (7)). Using only submatrices instead of the complete transformation is necessary, as it is impractical to apply thermal loads and to measure temperatures at each point within the structure. This is a common procedure in the field of structural vibration and it is possible to decouple the considered modes (see [16, 19]). However, the modes not taken into account in the transformation can be excited and their amplitudes recorded as a disturbance during the measurement. This phenomenon, which is known as spillover, is clearly described in [19].

For the following considerations, the coupling with the unobserved modes is neglected and regarded as an external disturbance of the system ($\bar{\theta}_{\mathrm{C},i} \approx \theta_{\mathrm{C},i}$). Under this assumption, (3) and (4) can be written as follows, considering only the controlled modes $\boldsymbol{\theta}_{\mathrm{C}}$ the inputs $\boldsymbol{q}_{\mathrm{A}}$ and outputs $\boldsymbol{T}_{\mathrm{S}}$:

$$\boldsymbol{\Gamma}_C\left(\dot{\boldsymbol{\theta}}_C + \boldsymbol{\Lambda}_C\boldsymbol{\theta}_C\right) = \boldsymbol{\xi}_C = \boldsymbol{\Phi}_{C,A}^T\boldsymbol{q}_A, \tag{13}$$

$$\boldsymbol{T}_S = \boldsymbol{\Phi}_{C,S}\boldsymbol{\theta}_C\,. \tag{14}$$

The application of equations (11), (12) and the modal controller (8), (13) and (14) results in independent equations

$$\gamma_i\left(\theta_{C,i}s + \lambda_i\theta_{C,i}\right) = \xi_{C,i} = k_{P,i}\left(\theta_{SP,i} - \theta_{C,i}\right) + \frac{k_{I,i}}{s}\left(\theta_{SP,i} - \theta_{C,i}\right), \tag{15}$$

where s represents the Laplace variable. From (15), the transfer functions of the controlled modes can be derived:

$$\frac{\theta_{C,i}}{\theta_{SP,i}} = \frac{k_{I,i}/\lambda_i\left(1 + s\,k_{P,i}/k_{I,i}\right)}{s(1 + s\,\lambda_i/\gamma_i) + k_{I,i}/\lambda_i\left(1 + s\,k_{P,i}/k_{I,i}\right)}, \tag{16}$$

5. SIMULATION

The transient simulation uses 16 thermal actuators and 16 sensors. These correspond to the areas F1 to F6, B1 to B6, L1, L2, R1 and R2 from Fig. 2. The first 16 modes with the largest time constants are used to calculate the transformation matrices in (10) and (12). However, for demonstration purposes, only four of the modal controllers are actively used. They are chosen so that one of the deformation degrees of freedom of the reference point *P* is significantly influenced. The modes are $i = 1$ for influencing u_{z}, 3 for u_{x} and 4 and 5 for u_{y} (see Fig. 6). The control of the first mode also serves to reduce the total amount of heat. All controllers are parameterised in the same way and are dependent only on the parameters of the corresponding mode:

$$k_{P,i} = \frac{\gamma_i}{\tau_{C,i}}\ and\ k_{I,i} = \frac{\gamma_i\,\lambda_i}{\tau_{C,i}}\,. \tag{17}$$

This leads to the following simplification of (5):

$$\frac{\theta_i}{\theta_{SP,i}} = \frac{k_{I,i}/(\gamma_i\,\lambda_i)}{s + k_{I,i}/(\gamma_i\,\lambda_i)} = \frac{1}{1 + s\tau_{C,i}}\,. \tag{18}$$

The time constant $\tau_{C,i}$ is a parameter that can be freely defined for the control system. It is chosen to have a value of $\tau_{C,i} = 0.125\tau_i$ for all modes. This leads to an asymptotic convergence to the target value, whereby the control time constant $\tau_{C,i}$ is derived from the modal time constant τ_i of the system.

A thermal load of 50 W is applied to the surface R2 and the two guides G1 and G2. This scenario is used primarily for visualisation purposes to induce deformations in different dimensions. There are no mechanical loads. The four modal controllers are initially inactive and are switched on successively at fixed times. The following Fig. 7 shows the displacement of point *P* as a result of the simulation.

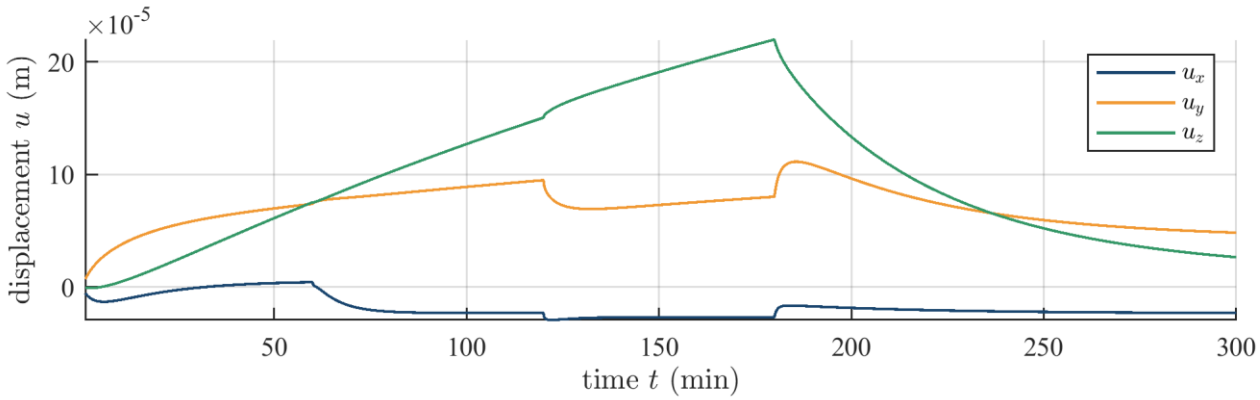

Fig. 7. Displacement of the reference point *P* in the transient simulation

The controller for mode 3 is activated after 60 min. The diagram shows that it is mainly the value u_x that changes at this time and that there is no influence on the other directions. At a time of 120 min, modal controllers 4 and 5 are activated. Although the value of u_y is mainly influenced, u_x and u_z are also influenced to a small extent. This is due to the fact that these modes influence all three displacement components of point *P*, as can be seen in Fig 6. A similar situation occurs when the first modal controller is activated at time 180 min, essentially reducing the amplitude of u_z. At the end of the simulation it can be seen that the three degrees of freedom of the deformation are stabilised, but a residual deformation remains. This is to be expected as the deformation components of the uncontrolled modes are not taken into account.

6. CONCLUSION

This contribution has presented a strategy for reducing the thermal distortion of a machine component. This is based on modal control of the temperature field using thermal actuators. If a thermo-elastic model of the structure is already available, the parametrisation is very simple. In the simulation, only a single parameter $\tau_{C,i}/\tau_i = 0.125$ was chosen, which is the same for all modes. All other necessary parameters and matrices can be obtained automatically from the model. It was also shown that individual degrees of freedom

in the state space can be specifically influenced. The concept presented thus offers the advantage of being able to systematically compensate deformations.

In the simulation shown, the deformation of point *P* was not fully compensated. To achieve this, the modal control concept presented will need to be refined in the future. Possibilities include, for example, increasing the number of modal controllers or estimating the deformation more accurately for better compensation. The use of a state observer is suitable for this purpose. This will be complemented by a detailed analysis of the spill over problem in the context of thermal systems.

When modelling the actuators, it was assumed that positive and negative heat flows could be set as required. In the next planned experimental studies on this strategy, heating elements will be used to stabilise the modal temperature gradients. The mean temperature can be reduced by overall cooling. This way of thermal load application is only used for basic research and is not suitable for practical applications. It would be preferable to use cooling circuits that can be independently controlled in this context.

ACKNOWLEDGEMENTS

This research was supported by a German Research Foundation (DFG) grant, received within the research project "Fundamental investigation of the modal control of temperature fields with the application on machine tool structures" (468584574), which is gratefully acknowledged.

REFERENCES

[1] MAYR J., et al., 2012, *Thermal Issues in Machine Tools*, CIRP Annals, 61/2, 771–791, https://doi.org/10.1016/j.cirp.2012.05.008.

[2] SCHROEDER S., GALANT A., KAUSCHINGER B., BEITELSCHMIDT M., 2018, *Efficient Modelling and Computation of Structure-Variable Thermal Behaviour of Machine Tools*, Conference on Thermal Issues in Machine Tools, 2018, 13–22.

[3] WECK M. et al., 1995, *Reduction and Compensation of Thermal Errors in Machine Tools*, CIRP Annals, 44/2, 589–598, https://doi.org/10.1016/S0007-8506(07)60506-X.

[4] KAUSCHINGER B., SCHROEDER S., 2014, *Methods to Design the Adjustment of Parameters for Thermal Machine-Tool Models*, Advanced Materials Research, Trans Tech Publications, Ltd., 1018, 403–410.

[5] CHEN J., YUAN S., NI J., 1996, *Thermal Error Modelling for Real-Time Error Compensation*, The International Journal of Advanced Manufacturing Technology, Springer Science and Business Media LLC, 12, 266–275.

[6] ZHU J., NI J., SHIH A.J., 1971, *Robust Machine Tool Thermal Error Modeling Through Thermal Mode Concept*, Journal of Manufacturing Science and Engineering, ASME International, 130, 0610061-0610069.

[7] MARES M., HOREJS O., HORNYCH J., SMOLIK J., 2013, *Robustness and Portability of Machine Tool Thermal Error Compensation Model Based on Control of Participating Thermal Sources*, Journal of Machine Engineering, 13, 24–36.

[8] FRASER S., ATTIA M.H., OSMAN M.O.M., 1999, *Modelling, Identification and Control of Thermal Deformation of Machine Tool Structures, Part 4: A Multi-Variable Closed-Loop Control System*, Journal of Manufacturing Science and Engineering, ASME International, 121, 509–551.

[9] HATAMURA Y., NAGAO T., MITSUISHI M., KATO K., TAGUCHI S., OKUMURA T., NAKAGAWA G., SUGISHITA H., 1993, *Development of an Intelligent Machining Center Incorporating Active Compensation for Thermal Distortion*, CIRP Annals – Manufacturing Technology, Elsevier BV, 42, 549–552.

[10] LI J.W., ZHANG W.J., YANG G.S., TU S.D., CHEN X.B., 2008, *Thermal-Error Modeling for Complex Physical Systems: The-State-of-Arts Review*, The International Journal of Advanced Manufacturing Technology, Springer Science and Business Media LLC, 42, 168–179.

[11] MATSUO M., YASUI T., INAMURA T., MATSUMURA M., 1986, *High-Speed Test of Thermal Effects for a Machine-Tool Structure Based on Modal Analysis*, Precision Engineering, Elsevier BV, 8, 72–78.
[12] BUENO R., ARZAMENDI J., ALMANDOZ X., 1997, *Thermal Modal Analysis and Modelling of Machine-Tools*, Integrated Design and Manufacturing in Mechanical Engineering, Springer Netherlands, 307–315.
[13] MARES M., HOREJS O., HORNYCH J., KOHUT P., 2011, *Compensation of Machine Tool Angular Thermal Errors Using Controlled Internal Heat Sources*, Journal of Machine Engineering, 11/4, 78–90.
[14] MORISHIMA T., VAN OSTAYEN R., VAN EIJK J., SCHMIDT R.H.M., 2015, *Thermal Displacement Error Compensation in Temperature Domain*, Precision Engineering, Elsevier BV, 42, 66–72.
[15] PREUMONT A., 2018, *Vibration Control of Active Structures*, Springer International Publishing
[16] MEIROVITCH L., BARUH H., 1985, *The Implementation of Modal Filters for Control of Structures*, Journal of Guidance, Control and Dynamics, 8, 707–716.
[17] PEUKERT C., PÖHLMANN P., MERX M., MÜLLER J., IHLENFELDT S., 2019, *Investigation of Local and Modal Based Active Vibration Control Strategies on the Example of an Elastic System*, Journal of Machine Engineering, 19/2, 32–45.
[18] PÖHLMANN P., PEUKERT C., MERX M., MÜLLER J., IHLENFELDT S., 2020, *Compliant Joints for the Improvement of the Dynamic Behaviour of a Gantry Stage with Direct Drives*, Journal of Machine Engineering, 20/3, 17–29.
[19] BRAGHIN F., CINQUEMANI S., RESTA F., 2012, *A New Approach to the Synthesis of Modal Control Laws in Active Structural Vibration Control*, Journal of Vibration and Control, 19, 163–182
[20] POPKEN J., SHABI L., WEBER J., WEBER J., 2018, *System Modelling and Control Concepts of Different Cooling System Structures for Machine Tools*, Conference on Thermal Issues in Machine Tools – proceedings, 93–106